Supplementary Material for "Detachment of giant liposomes - coupling of receptor mobility and membrane shape"

Hannes Witt,[a] Marian Vache,[b] Andrea Cordes,[b] and Andreas Janshoff[b]

[a] *Max Planck Institute for Dynamics and Self-Organization, Am Faßberg 17,37077 Göttingen, Germany.*
[b] *Institute of Physical Chemistry, Tammannstr. 6, 37077 Goettingen, Germany. Tel: 49 551 3910633; E-mail: ajansho@gwdg.de*

1 Additional theory

1.1 Law of mass action for an adhesive contact mediated by specific bonds

In experiments, adhesion is often a slow process thus we assume that the contact angle at the border of the adhesion patch is equal to the local equilibrium value derived from the Young's equation. We refer to this as the quasi-static regime.

In the following section we derive an expression for the free energy change ΔF arising due to formation of bonds between ligands present on the GUV and receptors displayed by the solid supported lipid bilayer. N_{LR} is the number of bonds formed between ligands L and receptors R in the contact area A_{c}. $\Gamma_{\mathrm{LR}} = N_{\mathrm{LR}}/A_{\mathrm{c}}$ is the area concentration of bonds in this area. $\Gamma_{\mathrm{L}} = N_{\mathrm{L}}/A_0$ is the concentration of free ligands on the GUV with area $A_0 = 4\pi R_0^2$. The total concentration of ligands before binding is $\Gamma_{\mathrm{L},0} = N_{\mathrm{L},0}/A_0 = (N_{\mathrm{L}} + N_{\mathrm{LR}})/A_0$. $N_{\mathrm{L},0}$ is the number of ligands on the GUV. On the apposing side, we have a concentration of unbound, free receptors $\Gamma_{\mathrm{R}} = N_{\mathrm{R}}/A_{\mathrm{plane}}$ on the solid supported lipid bilayer. Prior to binding we have $\Gamma_{\mathrm{R},0} = N_{\mathrm{R},0}/A_{\mathrm{plane}} = (N_{\mathrm{R,free}} + N_{\mathrm{LR}})/A_{\mathrm{plane}}$. The total free energy change upon formation of bonds in the contact zone is composed of three parts:

$$\Delta G = \Delta G_1 + \Delta G_2 + \Delta G_3 \tag{1}$$

ΔG_1 captures with the free energy change of the free ligands $N_{\mathrm{L}} = N_{\mathrm{L},0} - N_{\mathrm{LR}}$:

$$\Delta G_1 = (N_{\mathrm{L},0} - N_{\mathrm{LR}})(\mu_{\mathrm{L}}^0 + k_{\mathrm{B}}T\ln(\Gamma_{\mathrm{L}})) - N_{\mathrm{L},0}(\mu_{\mathrm{L}}^0 + k_{\mathrm{B}}T\ln(\Gamma_{\mathrm{L},0}) \tag{2}$$

and ΔG_2 the free energy change of the receptors, respectively:

$$\Delta G_2 = (N_{\mathrm{R},0} - N_{\mathrm{LR}})(\mu_{\mathrm{R}}^0 + k_{\mathrm{B}}T\ln(\Gamma_{\mathrm{R}})) - N_{\mathrm{R},0}(\mu_{\mathrm{R}}^0 + k_{\mathrm{B}}T\ln(\Gamma_{\mathrm{R},0}) \tag{3}$$

ΔG_3 is the free energy change due to formation of bonds:

$$\Delta G_3 = N_{\mathrm{LR}}(\mu_{\mathrm{LR}}^0 + k_{\mathrm{B}}T\ln(\Gamma_{\mathrm{LR}})) \tag{4}$$

At thermal equilibrium ΔG will be a minimum with respect to variations of N_{LR}. Therefore, we solve $\partial_{\mathrm{N_{LR}}}\Delta G = 0$ obtaining an equilibrium constant in analogy to the classical equilibrium constant for solution phase reactants:

$$K = \frac{\Gamma_{\mathrm{LR}}}{\Gamma_{\mathrm{L}}\Gamma_{\mathrm{R}}} = \exp\left\{\left(\frac{-\Delta G^0}{k_{\mathrm{B}}T}\right)\right\}. \tag{5}$$

Here, $\Delta G^0 = \mu_{\mathrm{LR}}^0 - \mu_{\mathrm{L}}^0 - \mu_{\mathrm{R}}^0 - k_{\mathrm{B}}T$. Not that in addition $k_{\mathrm{B}}T$ is subtracted from the chemical potential of the ligand-receptor bond.

1.2 Existence of inclination points in analytical force curves

The following paragraph shows that inclination points do not occur for

$$\widetilde{f} = \frac{\Psi \sin(\theta) - \Psi^2}{1 - (\Psi)^2}. \tag{6}$$

Setting $\frac{\partial^2 \widetilde{f}}{\partial \Psi^2} = 0$ we obtain for $0 < \Psi < 1$ real solutions only if they fulfil the condition:

$$\sin(\theta) = \frac{3\Psi^2 + 1}{\Psi^3 + 3\Psi}, \tag{7}$$

which exceeds the valid range for $0 \leq \sin(\theta) \leq 1$. Hence, no inflection points occur in force curves with $n = 2$. The situation is different if tension is not constant but contributions from area expansion add during deformation of the GUV. However, only numerical solutions exists for this case as shown in the main text. Inflection point occur already at $n = 2$ in this case.

1.3 Parameters used for calculations

Pretension	$T_0 = 0.1$ pN/nm
Area compressibility modulus	$K_A = 10$ pN/nm
Vesicle radius	$R = 7$ µm
Adhesion energy density towards the cantilever	$w_0 = 0.025$ pN/nm
Adhesion energy density towards the supported membrane	$w_0 = 0.01$ pN/nm
Adhesion energy density for the analytical solution	$w_0 = 10^{-5}$ pN/nm

2 Supporting figures

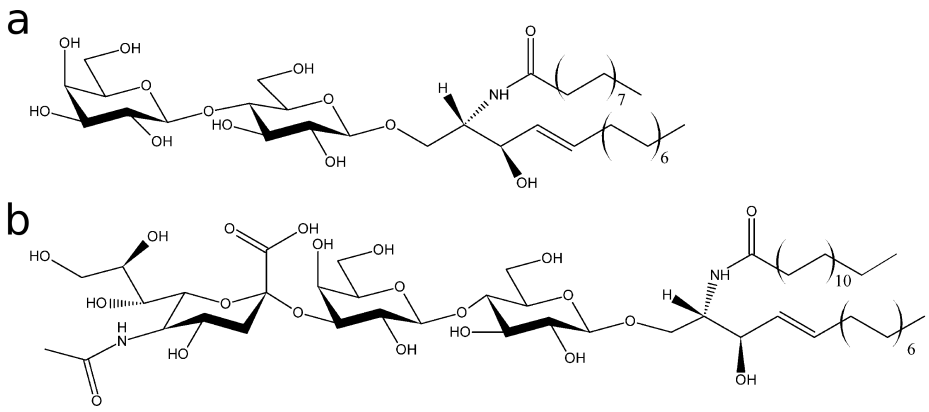

Figure S1: Structures of glycolipids used for adhesive interactions. **a** Lactosylceramide, **b** gangliosid G_{M3}. The structure of G_{M3} is only a representative out of a variety of possible structures present in the mixture.

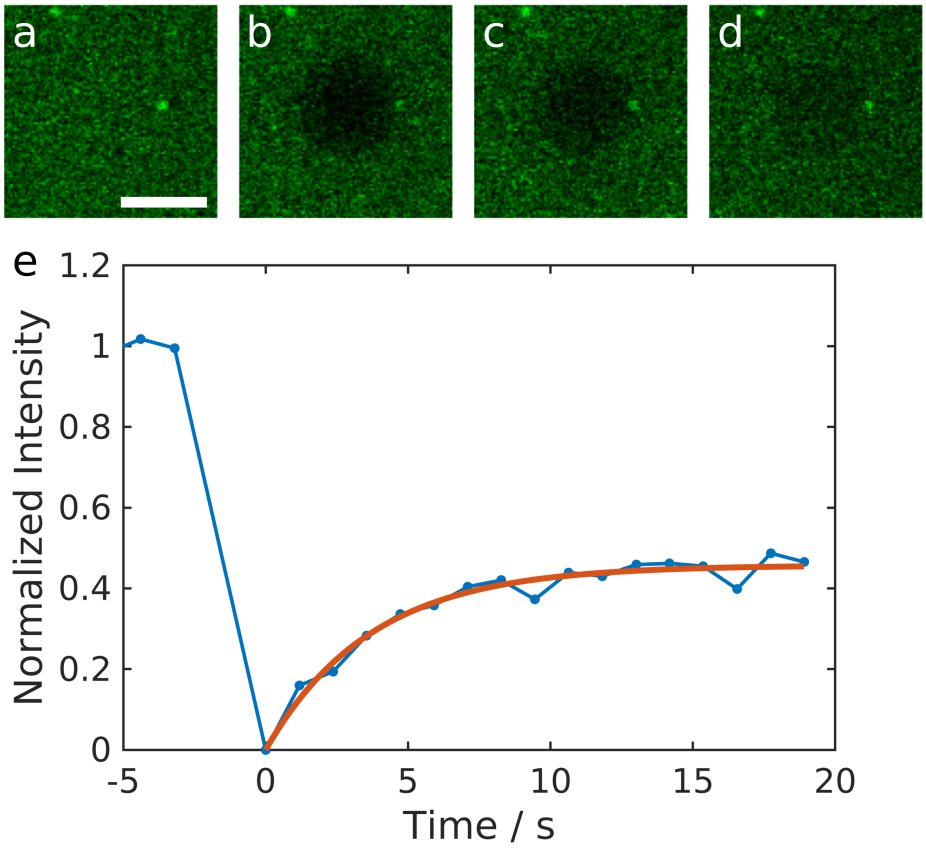

Figure S2: Fluorescence recovery after photobleaching experiment confirms mobility of SSM. **a** to **d** show confocal micrographs of the SSM, **a** before bleaching, **b** immediately after bleaching of the membrane dye (0 s), **c** 1.2 s after bleaching and **d** 19 s after bleaching. Scale bar 10 µm. **e** plots the fluorescence intensity against time (blue). The intensity was integrated over the whole region of interest, corrected for non-intentional bleaching by comparison with a close by reference region of interest and normalized to 1 before and to 0 immediately after bleaching. The red curve is a fit of the empirical function $I = P_{\mathrm{m}} \cdot (1 - \exp(-kt))$, where I is the normalized intensity, P_{m} the mobile fraction, k the time constant and t the time. The bleached circular area in **b** is partially refilled with fluorescent lipids within less than 20 s, confirming mobility of about 40% of the fluorescent lipids.

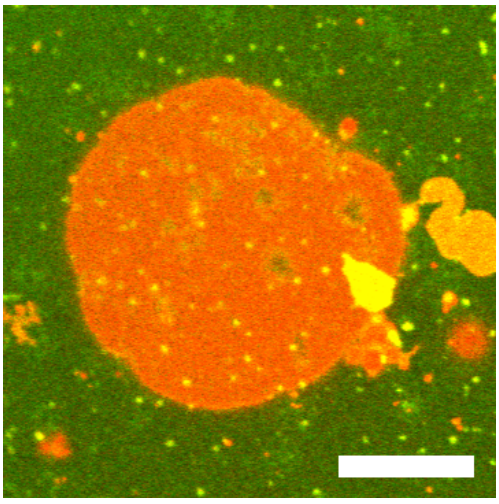

Figure S3: Confocal image of a GUV (red) firmly adhered to a solid supported membrane (green). The flat and continuous bottom plane of the vesicle indicates that the GUV is strongly adhered to the SSM rather than being loosely bond which would result in a smaller and discontinuous bottom plane due to fluctuations of the GUV membrane. Scale bar: 10 µm.

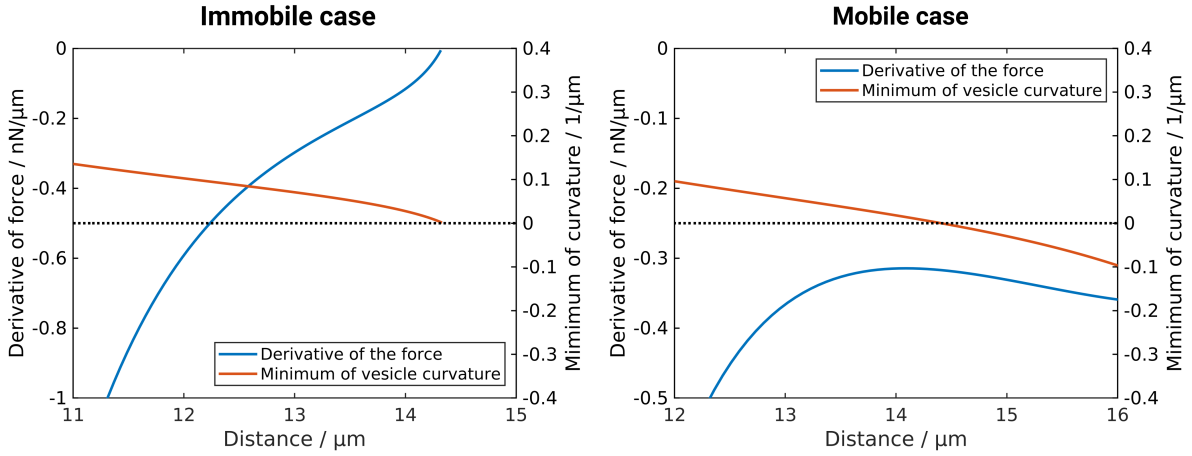

Figure S4: Comparison of the vesicle shape and the force-distance curve shape for the immobile case (left) and the mobile case (right). On the left axis the first derivative of the force $\mathrm{d}f/\mathrm{d}z$ is shown (blue). On the right axis the minimum of the curvature C_1 for each corresponding vesicle shape is shown (orange). The curvature can be calculated as $C_1 = \mathrm{d}U/\mathrm{d}r = a_i - b_i/r^2$. The minimum of C_1 is at $r = R_c$. As soon as C_1 is negative at any point of the vesicle, the vesicle assumes an unduloidal shape. Therefore, when the minimum of the curvature C_1 becomes negative, the shape transition from spherical to undoidal occurs. An extremum in the first derivative of the force indicates an infliction point in the force-distance curve. Note, that in the mobile case the maximum of the force derivative coincides with the zero-crossing of the vesicle curvature.

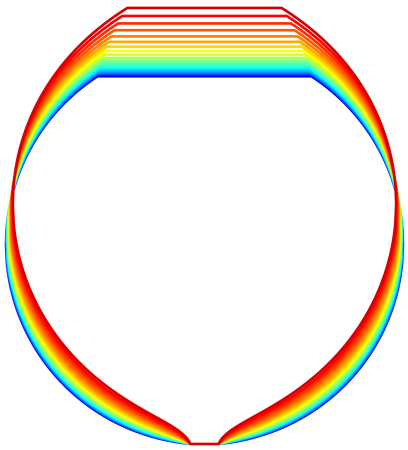

Figure S5: Non-physical generation of unduloidal vesicle shapes for immobile bonds. Vesicle shapes at a fixed lower contact radius $R_c = 0.5$ µm with adhesion energy densities increasing from $w_0 = 10^{-3}$ pN·nm^{-1} (blue) to $w_0 = 10^{-1}$ pN·nm^{-1} (red).

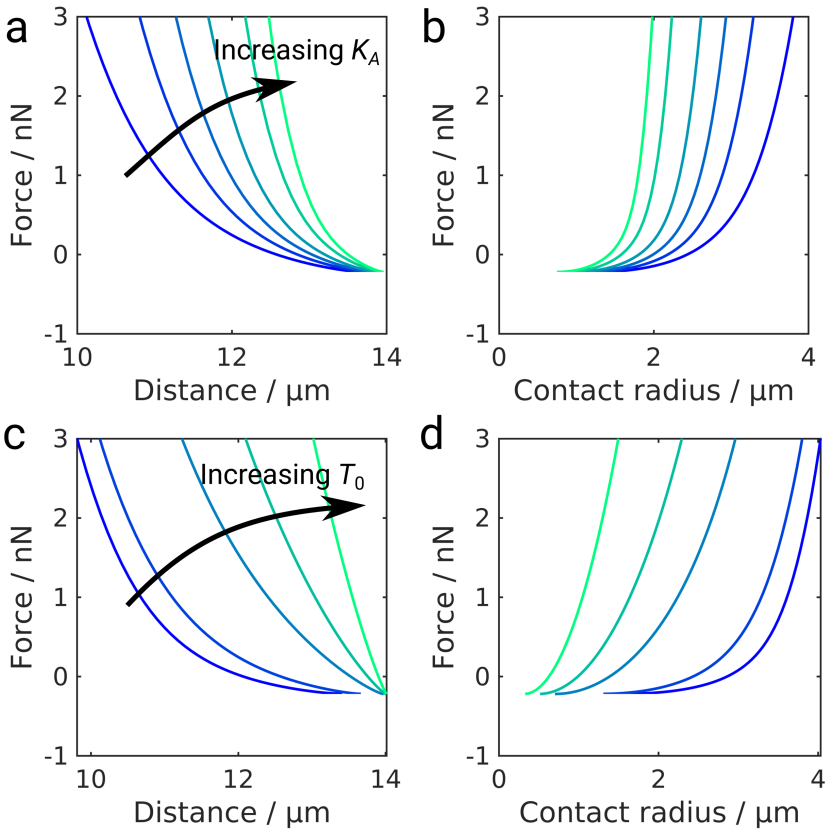

Figure S6: Impact of mechanical properties on GUV detachment for immobile bonds ($n = 0$). Force distance curves of GUV detachment calculated using the numerical model. **a** and **b** The area compressibility modulus is increasing from blue to green from 10 to 500 pN · nm^{-1}. **c** and **d** The pretension T_0 is increasing from blue to green from 0 to 2.5 pN · nm^{-1}.

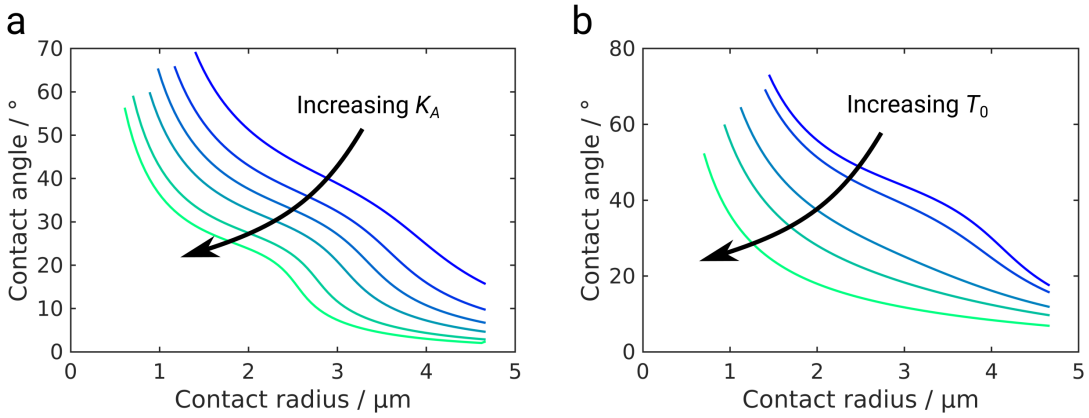

Figure S7: Impact of mechanical properties on GUV detachment for mobile bonds ($n = 2$). Contact angle as a function of the contact radius calculated using the numerical model. **a** The area compressibility modulus is increasing from blue to green from 10 to 500 pN · nm^{-1}. **b** The pretension T_0 is increasing from blue to green from 0 to 2.5 pN · nm^{-1}.

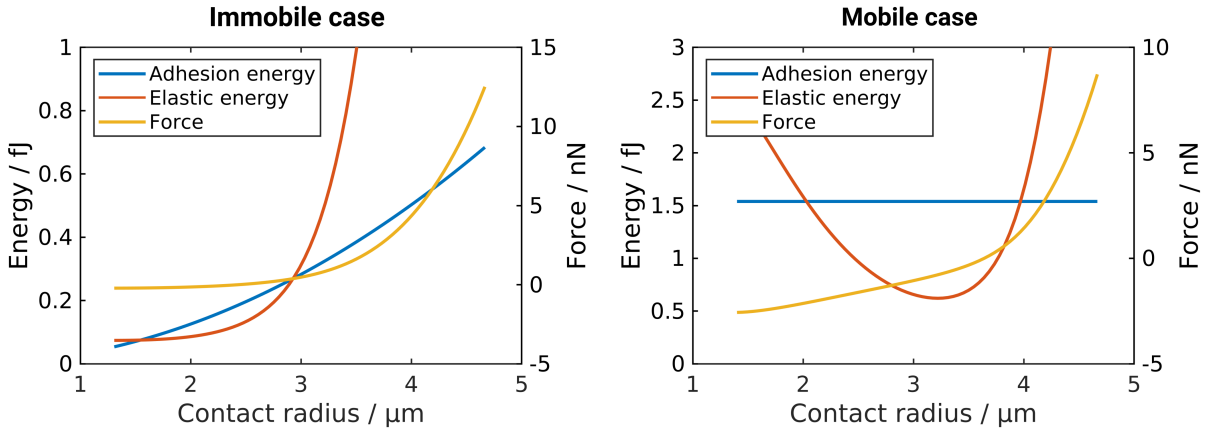

Figure S8: Adhesion energy (blue) and elastic energies (orange) for the immobile case (left) and the mobile case (right). The force (yellow) is shown on the right axis. Adhesion energy is calculated as $\pi w R_c^2$ and elastic energy as $0.5 K_A (A - A_0)^2 / A_0$.

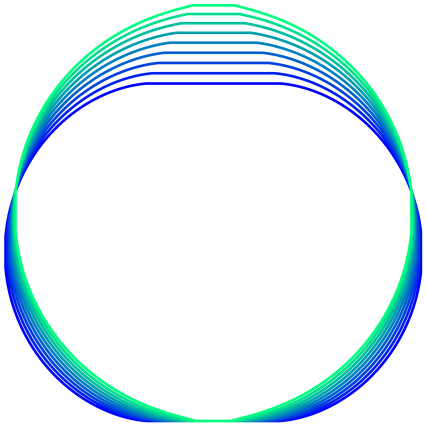

Figure S9: GUV shapes calculated using the numerical model for mobile bonds ($n = 2$) at very high tensions ($T_0 = 2.5$ pN $\cdot$ nm^{-1}). Increasing pulling forces are shown from blue to green. Note that the unduloidal shape typical for mobile bonds is not reached.

3 Supporting movie

The supporting movie shows a series of confocal fluorescent cross-sectional images recorded in the xz-plane during detachment of an adhered GUV by AFM. In each image, the corresponding force (F), the height (h) and the contact radius (R_c) are indicated. Fig. 1b in the main text was generated from images of this movie. 1 s in the video corresponds to 23.4 s in the experiment. The scale bar corresponds to 2 μm.